

Structural Critical Scattering and Magnetic Susceptibility Study of Zn-Doped CuGeO₃

Y. J. Wang, Y.-J. Kim, R. Christianson, S. C. LaMarra, F. C. Chou, R. J. Birgeneau

Department of Physics, and Center for Materials Science and Engineering, Massachusetts Institute of Technology, Cambridge, MA 02139

(December 2, 2024)

We report a comprehensive synchrotron x-ray scattering and magnetic susceptibility study of diluted spin-Peierls (SP) material Cu_{1-x}Zn_xGeO₃. Consistent with previously reported results on Mg-doped samples, we find similar phase behaviors in the Zn-doped case: the temperature at which the SP dimerization attains long-range order is significantly lower than the temperature at which the spin gap is established for doped samples, slow dynamics and Lorentzian squared intrinsic scattering lineshape are also found for the dimerization superlattice peaks in Zn-doped samples. In constructing the temperature versus concentration phase diagram, we find a critical concentration x_c ~ 2.35% for Zn-doped samples, above which only short-range ordered SP states are found for the whole temperature range we studied. In the complementary magnetic susceptibility study over the same samples, we observe the disappearance of the characteristic SP anomaly which indicates the absence of SP transition around the x_c determined by x-ray scattering, moreover, the low-temperature Néel transition cusp broadening is also confirmed in samples just above the x_c. By combining the information we collected from both synchrotron x-ray and magnetic susceptibility measurements, we clearly resolved the discrepancies reported in previous experiments by these two techniques. In interpreting the rich phase behavior exhibited by doped CuGeO₃, we use a heuristic phenomenological model which contains the impurity-induced competing interactions and the phase separation tendency upon the appearance of the Néel state.

PACS numbers: 75.30.Kz, 75.10.Jm, 75.40.Cx, 75.80.+q

I. INTRODUCTION

Low-dimensional quantum systems exhibit a variety of intriguing and often counter-intuitive properties. A prominent example of such a material is the spin-Peierls (SP) system¹¹ which consists of an array of one-dimensional (1D) antiferromagnetic spin-chains with S=1/2 on a deformable 3D lattice. Below the spin-Peierls transition temperature, T_{SP}, the spin-chains dimerize and a gap opens in the magnetic excitation spectrum. The discovery of an inorganic SP compound CuGeO₃¹ made possible a systematic study of impurity effects on SP systems². Despite extensive experimental and theoretical efforts devoted in studying the effects of dopants on the CuGeO₃ magnetic and structural phase transition²³⁴⁵⁶⁷, a lot of controversies still remain on all fronts. One major unresolved issue is the temperature versus concentration phase diagram. Zn doping, owing its relevance to High-T_c superconductivity studies, was by far the first and most studied dopant. An abundant information has been reported by all kinds of experimental techniques despite the fact that Zn turned out to be a 'bad' dopant later, we continue the study of Zn doping in hope by directly comparing our experimental results with all extant results, we can contribute one more piece of information to the understanding of this mysterious material.

Neutron-scattering on Cu_{1-x}Zn_xGeO₃⁸ revealed a phase diagram in which the T_{SP} first decreased linearly with the doping concentration and then started to show a

plateau-like behavior above 2% Zn doping. The plateau was presumed to persist up to more than 5% Zn doping. However, serious broadening on the SP excitations was detected in a 3.2% Zn-doped sample which suggested the existence of short-range ordered SP phase only. Susceptibility measurements², on the other hand, provided a different phase diagram. Below 2% Zn, susceptibility measurement agrees with neutron scattering on the linear suppression of the T_{SP}. However, above 2% Zn doping, susceptibility measurement reported no trace of SP phase transition, which was demonstrated by the disappearance of the characteristic dip in the susceptibility curve. Recalling our recent results on the Mg-doped samples, we find this discrepancy remains to be a general phenomenon for Cu-site doping studies of CuGeO₃. In the study of Mg-doped CuGeO₃, susceptibility measurement⁹ showed an abrupt disappearance of the SP phase above 2.3% Mg doping, while both x-ray and neutron have detected substantial scattering intensity from the SP phase¹²¹⁷ in the same doping range. Furthermore, x-ray scattering has found the SP phase ceased to be LRO around 2.1% Mg doping, agreeing within errors with the critical doping concentration determined by susceptibility measurement.

The discrepancy was then partially resolved by the complementary information provided by both techniques. However, interesting questions arise on the physical origin of this seemingly inconsistent picture. In this paper, we present a comprehensive x-ray scattering and magnetic susceptibility study of the Zn-doped CuGeO₃. By

using the experimental results obtained on the same samples by two techniques, we can clearly pinpoint the origin of the previous discrepancy, a theoretical spin-glass model is then proposed to explain our experimental results.

II. EXPERIMENTAL CONDITIONS

A. Sample preparation

A series of high quality single crystals $\text{Cu}_{1-x}\text{Zn}_x\text{GeO}_3$ are grown by travelling floating-zone methods. The crystals are grown over seed single crystals with 100ml/min O_2 flow to reduce oxygen loss. Samples have a typical mosaic spread less than 0.05° at major Bragg diffraction peaks. Since typical x-ray penetration depth of CuGeO_3 crystal is of several microns, it can only probe the properties of near surface layers. EPMA method was then used to determine the doping concentrations. We believe it can yield more relevant information since EPMA is also a surface technique. The typical sample size both used for x-ray scattering and magnetic susceptibility measurements is about $3 \times 3 \times 1\text{mm}^3$. Twenty evenly spaced spots covering the whole sample surface are used in EPMA measurement. The variation of concentrations are recorded as the uncertainties of the sample concentration. We summarize the sample characterization results in Table I. As shown in Table I, the actual Zn contents are always lower than the nominal ones in high doping range, which is consistent with previously reported results^{8,16}. However, despite the great disparities between these two concentrations, the concentration gradients and fluctuations along the surface remains relatively small and comparable to the Mg case⁹. Moreover, the concentration variations have similar magnitudes for all samples, which would suggest a similar influence over the SP phase transition.

As would be discussed in detail, we believe there exists intrinsic mechanism which is responsible for all kinds of unconventional characteristics of the SP phase transition in doped CuGeO_3 instead of simple concentration gradients, so a detailed and careful characterization of the samples remains crucial. We prepare our samples by cutting them from the end of regular growths which have lengths over 5cm. We believe by doing so, we can effectively eliminate the gradient induced in crystal growth since we were using a different doping level crystal as the seed crystal.

B. SQUID magnetometer

The magnetic susceptibility measurements were done using commercial SQUID magnetometer (Quantum Design Inc.).

C. Synchrotron Beamline

The experiment was carried out at MIT-IBM beamline X20A at the National Synchrotron Light Source. The x-ray beam was focused by a mirror, monochromatized by a pair of Ge(111) crystals, scattered from the samples and analyzed by a Si(111) analyzer. The x-ray energy was set at 8.5 kev. Samples were carefully cleaved before placed inside a Be can filled with helium heat-exchange gas and mounted on the cold finger of a 4K closed cycle cryostat. The experiment was carried out around the (1.5 1 1.5) SP dimerization peak position with the (H K H) zone in the scattering plane. The highest intrinsic correlation length resolvable in our experiment was about $0.5\mu\text{m}$. we considered that a sample possesses LRO if the correlation length exceed this value since significantly larger length are essentially macroscopic.

III. EXPERIMENTAL DETAILS

A. Synchrotron x-ray scattering

Synchrotron x-ray scattering has long been proven to be a versatile tool in studying structural phase transitions. X-ray can detect critical fluctuations as well as the long range order. Using the knowledge gained from x-ray scattering near the phase transition, we can construct several critical exponents associated with the phase transition which can inform us of the exact nature of the transition itself. Owing to its high flux and high reciprocal space resolution, synchrotron x-ray scattering can have more advantages over other techniques in resolving subtle issues and revealing new physics which would be otherwise simply ignored by other techniques. Our first approach to tackle the doped CuGeO_3 problem was straightforward, just simply replicating what we and other people have done on undoped CuGeO_3 and later we can interpret our data in a comparative sense. Although there still remains some discrepancies on the interpretation of the SP transition in undoped CuGeO_3 , sufficient data supports the claim that it is a well defined second order phase transition, for x-ray scattering, this is evidenced by order parameter and critical fluctuation studies. In the following, we would begin to present our experimental results on the doped samples and show how do them deviate from our original expectations.

Fig. 1(a) shows the temperature dependence of the (1.5 1 1.5) dimerization peak intensity for various Zn-doping samples. We have attempted to normalize the data with the corresponding (1 0 1) Bragg peak intensity. However, we can not achieve any systematically behaved results as in Mg doped case¹². The data are then normalized to its own peak intensity at 5K instead. In sharp contrast to the undoped CuGeO_3 , the transitions for doped samples are noticeably rounded with the

rounding increases with increasing doping. Such a substantial rounding cannot be simply explained by local concentration gradient since the doping is too low to create any correlated effect²¹ and also because the experimentally checked concentration gradient remains same magnitude for most samples. In 3D random systems, it is always important to determine with certainty whether the transition smearing is due to macroscopic concentration fluctuation or is intrinsic to the physics. As is evident from the figure, We can see there exists a clear pattern for the rounding of the order parameter to increase from undoped to highly doped samples.

According to Table. 1, the 3.8% Zn-doped sample has concentration variance less than 0.2%, while the order parameter goes up at a gentle slope without saturation for the whole temperature we studied. It would be far-fetched then to attribute the nearly flat order parameter being to concentration gradient, on the other hand, the increasing rounding would inevitably require explanation from some intrinsic physics.

Not only does the order parameter changes drastically upon doping, the corresponding correlation length also behaves largely different with the undoped sample. Fig. 1(b) shows the temperature dependence of the longitudinal inverse correlation length for different doping samples. The minimum inverse correlation length which the system can achieve as a function of x is shown in the inset. A similar figure as in the Mg case has been obtained¹². Again, unlike the undoped sample, in which the inverse correlation length decreases rapidly as approaching T_{SP} from above and plummets to 0 at T_{SP} . The inverse correlation length curves for doped samples take a much milder way in approaching LRO, that is to say, the curves approaches zero in an asymptotic way without clear sign of the exact temperature it hits zero. This complication makes a unequivocal determination of the T_{SP} difficult. As we should see in below, the same difficulty appears as we try to determine the critical concentration along the doping axis. Based on the maximum correlation determined to our experimental accuracy, the system attains LRO only for $x \cong 0.0235$, while substantial intensity are still observed at the superlattice peak positions for $x=0.0255$ and 0.027 samples which have $x > x_c$, despite that the scattering peaks cease to be resolution-limited. The x_c we determined for Zn-doped is slightly higher than that for the Mg-doped case. This could be simply due to the different techniques used in determining concentration, ICP⁹ for Mg and EMPA for Zn, or it is intrinsic as we stated above.

B. Susceptibility

Magnetic susceptibility of the same samples used in synchrotron experiments has been measured using SQUID magnetometer. Samples were mounted with the c axis parallel to the applied magnetic field, the data

were taken in a magnetic field of 500Oe. Fig. 2 shows the temperature dependence of susceptibility of all measured samples. The overall features are similar to previously reported results¹⁵⁹¹⁸:rapid suppression of the SP phase upon doping and the appearance of a low temperature Néel ordering. Analogous to dimerization order parameter measurement, the kink anomaly which is characteristic of SP transition is much smoother and more rounded for doped samples in comparison to undoped CuGeO₃. We determine T_{SP} of the susceptibility measurement from the maximum of the derivative of the kink anomaly and $T_{Néel}$ simply from the low temperature cusp position. The main purpose of our susceptibility measurement is to give supplemental information to our synchrotron x-ray studies, in doing so, we can gain a more complete understanding of doped CuGeO₃. Bearing this picture in mind, we then focus our attention on samples which show unconventional characters in synchrotron x-ray experiments. Fig. 3 shows the temperature susceptibility measurements for four samples around critical concentration determined from x-ray experiment. Samples with $x=0.0235, 0.0255, 0.034$ have single low-temperature cusp which is usual when Néel transition sets in. The interesting feature lies in $x=0.027$ sample, the susceptibility curve of $x=0.027$ sample of has a dip at high temperature which is characteristic for a SP transition. Besides, there exists one broad low temperature cusp where the Néel transition is supposed to be. This is reminiscent of similar results in Mg-doped case, Masuda *et al.*¹⁸ did susceptibility experiments on a series of Mg-doped CuGeO₃, and they found a double peak feature in low temperature susceptibility curve which was ascribed as two Néel transitions. The double peak feature spans the concentration from $x_{c1}=0.0237$ to $x_{c2}=0.0271$, which is far beyond the concentration fluctuation 0.001 determined in Mg-doped case, a simple concentration gradient effect to explain the usual broadening would be inadequate. On the other hand, interesting questions arise on what is the true cause of this unusual broadening. Si-doped samples have been measured by susceptibility experiments too, the qualitative difference between Si- and Mg- doping studies lies in whether there exists two Néel transitions or just a broadened Néel transition¹⁸¹⁵. Since Zn, Mg, and Si have all been proven to be well-controlled dopants, the existence of the broadening or two-peak feature has long raised question on its origin¹⁸¹⁵. Masuda⁹ interpreted it as a first order phase transition between D-AF to U-AF phase for Mg-doped samples while not for Si-doped case. In this paper, an alternative explanation is given which can explain the occurrence of the broadening equally satisfactorily. As would be clarified in detail later, We believe the broadening of the low-temperature Néel transition is closely related to the re-entrance of the SP phase and the key lies in the inhomogeneous nature of both the SP and Néel phase. Coming back to the experimental results, if we compare numerical details of the susceptibility measurement of Zn- and Mg- doped samples, we find more

striking similarities. The sample which has the highest Mg-doping level without showing the broadening feature has a Néel transition around 2.9K with $x=0.0229$, then starting from $x = 0.0237$, there exists a broadened cusp spanning from 3.2K to 3.9K, the cusp was peaked more to the left side with the weight gradually shifting to the right as the concentration increases¹⁸. In Fig2(b) we can find similar behavior with $x = 0.0255$ Zn-doped sample shows a single cusp at 2.9K and $x = 0.027$ sample showing a broadened cusp ranging from 3.1K to 3.8K, the left side of the cusp is much higher than the right side suggesting it is near the lower concentration boundary of the broadening peak phenomenon. Unfortunately, we don't have intermediate doping concentration samples from $x=0.027$ to $x=0.034$ which can give us a complete view of the gradual shift of the weight change. The important point is we confirmed again the regime where susceptibility shows serious broadening coincides with where SP begins to lose LRO while substantial intensity is still observable¹². So the Néel transition broadening is then directly correlated with the loss of LRO of SP phase. It has long been found the Néel transition in doped CuGeO₃ had unusual characters, neutron experiment on 3.4% Zn-doped CuGeO₃² revealed that unlike a typical Néel transition, the order parameter wasn't saturated even at 1.4K, also the transition itself was considerably rounded. Fitting the order parameter using a Gaussian distribution of the transition temperature, they got $\beta = 0.22 \pm 0.02$ which doesn't fit in any 3D universality class. Even more surprisingly, the Néel order turned out to be LRO. μ SR³² reported the Néel ordering process was an inhomogeneous process with islands of freezing spins start to appear from the paramagnetic phase, although the transition was 'mistakenly' interpreted in a spin glass picture, it revealed the Néel transition wasn't a homogenous process despite the fact it was LRO. As would be discussed in detail in theoretical understanding section, we pointed out the inhomogeneous ordering of the Néel transition is due to the inhomogeneous SP phase and even a possible phase separation process.

C. Phase diagram

The phase diagram of Cu_{1-x}Zn_xGeO₃ is revisited by both synchrotron x-ray and susceptibility measurement. One obvious motivation for this work is to resolve the drastically different phase diagrams reported⁸² by different groups. Minor beam heating problem has been addressed in our experiment which results in perfect agreement of T_{SP} determined for undoped CuGeO₃ by both x-ray and susceptibility measurements. We define two characteristic temperatures, both related to the SP transition but defined by the physics on different length-scales. The higher transition temperature T_m, defined as the temperature corresponding to the maximum of critical fluctuations which is measured as the wing inten-

sity of dimerization peak. We define the counterpart of T_m for the susceptibility measurement at the maximum of the derivative of the susceptibility, $d\chi/dT$, which has a similar physical significance as the maximum of the critical fluctuation. The lower transition temperature T_S is defined as the temperature when the lattice dimerization achieves LRO, *i.e.*when correlation length goes to infinity. As we can see in Fig. 4, there is no ambiguity in the definition of T_{SP} as far as undoped CuGeO₃ is concerned: the superlattice peak intensity plunges to zero at 14.1K while corresponding correlation length diverges precipitously at the same temperature. In the inset, we show the intensity at the wing($\delta q = 2.1 \times 10^{-3} \text{ \AA}^{-1}$) of the dimerization peak which corresponds to the critical fluctuation. It is clear that the critical fluctuation reaches maximum at 14.1K too. Keeping the definition of second order phase transition in mind, we can safely draw the conclusion that T_{SP} = 14.1K. Susceptibility on the same sample doesn't yield any contradictory result. A sharp kink anomaly is observed at 14.1K. When taken the derivative, there also exists a sharp λ -like cusp with maximum at the same temperature. Since a SP transition can be either defined as the opening of the gap in the magnetic excitation spectrum or the appearance of the lattice dimerization, the perfect agreement by two different techniques proves SP transition to be well-defined second order phase transition and the equivalence of two transition temperature definitions. Physically it means the magnetic gap opening coincide with the dimerization achieving long-range coherence.

Discrepancy develops between these two definitions as we go into the doped regime. It is then difficult to define unambiguously T_{SP}. As illustrated in Fig. 5, we show the experimental results on $x=0.0235$ sample. In the upper panel, we find the onset of the order parameter is seriously rounded, substantial intensity starts to appear as high as 10K and the fluctuation reaches maximum around 9.3K. At the same time, we notice the correlation length doesn't diverge until as low as 7K. In the bottom panel, we show the magnetic susceptibility measurement on the same temperature scale. We find the kink anomaly corresponding to the SP transition has been smoothed out and the derivative of susceptibility gives a rounded peak around 9.5K. If a linear extrapolation method has been exploited to define T_{SP}, we can get a even higher T_{SP} at about 10K. These seemingly contradictory results in some sense can partially explain why there exist all kinds of different doping phase diagrams.

To illustrate the discrepancy more clearly, we recall we define T_S as the temperature where the correlation length diverges. Applying the same criteria to doped samples, as obvious from the definition, naturally we are going to get a much lower phase transition temperature than from other definitions. In Fig. 6, we plot the new phase boundary in conjunction with the susceptibility results by both definitions. Our phase diagram is in several ways distinctive: the phase boundaries determined by different definitions of T_{SP} do not match each

other except at $x=0$, with the divergence increase as the doping level increases. Using T_S to construct the phase diagram, we get a nearly vertical phase boundary around $x=0.0235$ from synchrotron x-ray results, no SP LRO can be achieved above this concentration level, although substantial intensity from the dimerization peak is still observable. This effect is most pronounced for 2.7% Zn-doped sample which we can observe non-negligible broadening of the dimerization peak even at 4K while the peak remains strong. 2.7% is also the doping level, we believe not accidentally, where the broadening of the Néel transition in susceptibility measurement is clearly observed. Using T_m , on the other hand, we end up with a rather different phase diagram, in which the T_m determined by synchrotron x-ray and magnetic susceptibility measurement follows an approximate linear suppression law upon doping. Especially for $x=0.034$, the sample doesn't achieve LRO for the whole temperature range we studied, thus no T_S can be defined in this way. On the other hand, we can still determine T_m because there still exists substantial intensity at the dimerization peak in certain temperature range and a subsequent peak in critical scattering is well defined. Furthermore, if we trust the linear suppression law would persist up to even higher doping levels, we find the extrapolated phase boundary to intersect with the doping axis around $x=0.06$, which would correspond to the doping level where even SRO SP phase is destroyed. In summary, as illustrated above, the seemingly contradictory phase diagram reported by different techniques in some sense is due to the complexity of the Phase diagram itself, thus an accurate determination of the phase diagram including both T_{SP} and x_c relies heavily on the full understanding of the underlying physics which we believe is highly nontrivial.

D. Unconventional phase transition

SP transition in doped samples has shown some unconventional characters. Besides the ambiguity in the determination of the T_{SP} and x_c , there exists other anomalies absent in a typical second-order phase transition. One of them is when the system undergoes a SP transition, it takes anomalous long relaxation time for the system to reach phase equilibrium, *i.e.*, the superlattice peak intensity keeps on changing monotonically in a course of several hours with the scattering peak width changes accordingly. It would cause serious thermal hysteresis in the order parameter measurement if the system were not kept sufficiently long after changing temperature. Several aspects of the slow dynamics are worth mentioning: first, the novel slow dynamics is absent in undoped CuGeO_3 , under the same experimental conditions, upon change of temperature for several degrees, the undoped system can achieve phase equilibrium within few minutes, in sharp contrast to the highly doped samples. We characterize the slow dynamics by sitting on top of the superlattice

peak and doing time scans while keeping the temperature constant. The time scan for system in equilibrium would show zigzag behavior with the centerline remaining flat. The zigzag behavior reflects the temperature fluctuation at the sample place and agrees well with the temperature fluctuation pattern recorded from the temperature controller. Fig. 7 shows the time scan for $x=0.0235$ for both heating and cooling runs. After the sample is cooled from 8K to 7K, it is observed that the peak intensity monotonically increases and doesn't saturate after more than half an hour. If we look closer enough, we can even notice the similar zigzag behavior which modulates the monotonic increase. This reveals that the slow dynamics is not caused by poor thermal contact. The slow dynamics is still prominent even upon change of temperature by 0.05K, as shown in upper panel of Fig. 7. We also tried to plot the intensity on a logarithmic scale. A linear relationship between the time and peak intensity on the logarithmic scale plot suggests that the peak intensity could be following some logarithmic behavior. We note that the linear relationship could be accidental because it would be necessary to monitor the behavior for three decades to draw any meaningful conclusion. Besides, upon the change of peak intensity, scattering peak width would change concomitantly. A slow increase of intensity is accompanied by slow decrease in peak width and *vice versa*. Surprisingly, the slow dynamics would be absent if system has already reached LRO and any further change of the temperature within the LRO regime would not induce slow dynamics. We do not have time scans for the dimerization peak width which exhibits how does the correlation of the system evolve with time. To track the evolution of the correlation length, we have to do full scans which would inevitably change the extant experimental conditions. The third aspect of the slow dynamics is that it is most prominent near the phase boundary, where considerable intensity has been observed although the phase itself hasn't achieved LRO, which roughly coincides with the regime between T_m and T_s . To understand the origin of slow dynamics, we first recall that for SP systems, the phase transition occurs when the neighboring spins pair up and create a local gap in the excitation spectrum and the LRO is achieved when the phase coherence of the local gap is established. In undoped CuGeO_3 , these two events happen at the same temperature. For doped samples, on the other hand, we observed substantial intensity while system is still SRO, which means SP order has been established locally although system has difficulty in achieving global phase coherence. The existence of the slow dynamics system normally suggests metastable behavior of the system.

We recall thermal hysteresis or slow dynamics are common for systems with competing interactions or fields²⁰. Competing interactions or fields create multi-minima in the free energy landscape and makes true ground state elusive when the system undergoes phase transition. The system has to overcome numerous local energy barriers and can easily fall out of equilibrium by trapped inside a

metastable state. The slow dynamics in doped CuGeO₃ resembles similar behavior in random field Ising model system²⁰. As we would clarify later that we believe this resemblance is not coincidental and bears direct relevance to the competing interactions caused by doping.

E. Line Shape

Owing to small mosaic spreads ($\leq 0.05^\circ$) of the single crystals and high brightness of the synchrotron x-ray($\sim 10^{11}$ photons/sec), we can always get as much as more than 50,000 counts/s at the dimerization peak for low doping samples where SP phase has not been strongly suppressed. The scattering geometry includes double bouncing Ge(111) monochrometer and Si(111) analyzer, the typical backgrounds are less than 10 counts/s. The low statistical error owing to the high intensity and high signal to background ratio can give us unique opportunity in determining the correlation length and line-shape with much higher accuracy compared to neutron scattering. In extracting the correlation length, the resolution function is experimentally measured at (3 0 0) Bragg peak which has a rather close Q vector in reciprocal space with (1.5 1 1.5) dimerization peak. When the resolution function is used to extract the correaltion length of undoped CuGeO₃, it results in an error above 5000 Å which we consider to be the upper limit of our experimental accuracy. The determination of the line-shape is further complicated by the existence of the two-length scale problem as has been discussed in our previous work¹³. Since two superimposed profiles are always present in critical scattering in the close vicinity of the SP transition for low doping samples, it makes our determination of intrinsic cross-section more difficult. However, only single scattering profile is observable experimentally in critical scattering for high doping samples, we would presume it is due to the dominance of dopants over dislocations which are causing the second length scale. For second order phase transitions, the critical scattering lineshape should have a Lorentzian character. So any deviation from it would provide ample information on the nature of underlying phase transition. In fig. 8 we show the low temperature superlattice peak scattering profile for SRO x=0.038 sample, apparently, resolution function is much narrower in comparison with the scattering profile, so the fitting results are insensitive to the precise form of the resolution function used. Both Lorentzian and Lorentzian squared cross section have been used to fit the data. The Lorentzian squared lineshape gives discernable better fitting result than simple Lorentzian lineshape. The existence of Lorentzian squared cross section instead of Lorentzian is significant because in a simple dilution induced percolation problem²⁰, even above the percolation threshold, the diffuse scattering is always Lorentzian in character, dilution simply sever the interaction paths between neighboring sites until there is no

longer an infinitely connected network, *i.e.* no LRO can be established above the percolation threshold. However, the cross section remains Lorentzian-like which is characteristic for thermal fluctuation. Usually, the occurrence of the Lorentzian squared lineshape implies random field or competing interaction dominant physics²⁰. In treating the doping problem of the CuGeO₃, the first thought would be drawing the analogy in a simple dilution problem. However, the Lorentzian squared lineshape would undermines a simple dilution induced percolation explanation of the destruction of the SP phase. As would be discussed in detail in section V, we believe the occurrence of the unexpected crosssection is closely related to the intrinsic competing interactions generated upon doping.

IV. CRITICAL SCATTERING

According to conventional knowledge of phase transitions, second order phase transitions can be categoized according to different universality classes, the difference of all universality classes is governed only by the spatial dimensionality and the number of the components of the order parameter, there also exists a set of critical exponents which are solely dependent on the universlity class. So by studing the critical exponents associated with certain universalityclass, we can gain a lot of insights into the phase properties. In this work, we measured the critical fluctuations of Zn-doped CuGeO₃, the results we obtained are striking. We noted here that even in the case of undoped CuGeO₃, there lacks a concensus over the universality class of the SP transition²⁰³³⁵. We resolved this conundrum by showing that the phase behavior in the vicinity of the phase transition can be quantitatively fitted with a mean field model incorporating a tricitical to mean field crossover²⁰. The issue of the relevant spatial dimensionality has also been discussed in our previous work¹³ where we presented our results on undoped CuGeO₃. In the top panel of Fig. 10, we show the order paramemter mesurement and the associated critical fluctuation intensity at the wing of scattering peak for 1% Zn doped CuGeO₃. The transition is slightly broadened as compared to the SP transition in undoped CuGeO₃. This is reflected both in the order paramemter smearing and the temperature range of the critical fluctuation. The marked difference in the critical scattering behavior with undoped CuGeO₃ is shown in the bottom panel. It is apparent that the ciritcal exponent associated with the correlation length is totally different from the undoped sample, the correlation length follows more or less a linear relationship with the temperature. Since the critical exponents for certain universality class are fixed by definition, the change of the critical exponet in the doped CuGeO₃ would suggest a change of the underlying universality class, which is quite astonishing noting the fact that there is only 1% of Zn being dopd inside. The effort to match the ciritcal exponent with existing

universality classes is also futile, as we know, for common 3D universality classes, the critical exponent ν is always less than 1. Notably, the determination of the transition temperature has become a problem by itself due to the serious transition rounding. Any uncertainty in the determined transition temperature would induce further difficulties in our discussion of the critical exponents since the the critical exponents is determined with respect to the reduced temperature where the absolute value of the transition temperature would be of direct relevance. Returning to the undoped CuGeO_3 , where the transition temeprature can be determined by the onset of the order parameter, the divergence of the correlation length or the maximum of the critical fluctuation intensity, the SP transition temperature difference determined in these ways are within $0.1K$. So when we are trying to extract the critical exponents , it would be less sensitive to the way we determine the transition temperature. This ceases to be trivial problem when the doped samples are concerned, the exponent we extracted are directly dependent on the way we determine the transition temperature. In this work, We are going to adopt the way of determining the maximum of the critical fluctuation partly due to the matching with the susceptibility measurement. We pointed out this is not a new issue we are facing. People study systems with competing interactions always encounter rounding due to intrinsic effects²⁰, the issue of determining the phase transition temperature has been subtle and under hot debate over years. We pointed out briefly here that different way of determing the transition temperature would inevitably chnage all our arguments below, but we emphasize the main idea we want to convey is to relate the doped CuGeO_3 phenomnology to the system with intrinsic competing interactions. In Fig. 11, we continue to present the results for 2% Zn-doped sample, we notice both the broadening in the order parameter and the diffuse scattering have incresed significantly. The correlation length , approaching the transition from above, first exhibits some linear realtionship with decreasing temperature, then, close to the transition, the rate of the divergence slows down and shows some kind of asymptotically slowing process in approaching the LRO, interestingly , if we extrapolates the linear behavior to intersect the temperature axis, we obtain a temperature which roughly match the maximum of the diffuse scattering, *i.e.* the phase transtion temperature. Obviously, we believe there also exist some narrow region close to the transition temperature for 1% Zn doped sample, in which the correlation length shows some kind of slowing down process. However, we note that the linear relationship between the correlation length and the temperature is most apparent in 1% Zn doped sample and extends down to very close vicinity of the transition temperature. Fig. 12 shows the similar results for 2.35% Zn doped sample. The asymptotically slowing down process is clearer in the sample, while it still obeys the qualitative observation that the extrapolation of the linear behavior meets the maximum of the diffuse scattering. Summing

up all the information we have obtained, we find it is reminiscent of similar behavior observed in random field systems²⁰. The difficulty in systematically studying systems with quenched randomness has always been on the control of randomnees inside of the system. To produce a series of samples in with the quenched randomness has a continous change could be extremely chanllenging. The problem has been solved by Fishman and Aharony¹⁹ in study of random field systems. They thorectically proved the equivalency of the Random field Ising system with the diluted antiferromagnetic sytem under uniform field, and the magnitude of the random field is determined by the uniform field applied on the system and hence forth can be varied continously. The random field system has then been extensively studied in the past years. One of the intriguing results in the critical scattering study of RFIM is there exists an extended region where the measured inverse correlation length varies linearly with the temperature with the extrapolation to infinite correlation length close to true transition temperature. Instead of a clear transition with the inverse correlation length follows some power law behavior, Similar asymptotical slowing down is also observed in the RFIM system, the resemblance in the critical scattering is a very strong evidence to prompt us to try to relate the doped CuGeO_3 with the well-studied RFIM system. As noted in other sections, additional evidences to connect the doped CuGeO_3 with the random field sytem has been found in anomolous slow dynamics, scattering lineshape. By combining all the relevant information and our theoretical understanding in the nature of the doping effect over the SP phase transition, we can reach a coherent picture in which the observed resemblance of these two systems are the natural result of the intrinsic competing interactions for the doping effect on SP transition.

V. THEORETICAL UNDERSTANDING

One question haunting doped CuGeO_3 problem is why SP phase can be destroyed by only 2% Zn doping or even less in Si case. Khomskii *et al.*⁶ exploited a soliton model which gives a suitable description for the doped CuGeO_3 . However, if we treat the destruction of the SP phase in a simple soliton dilution picture, it would naturally yield a critical concentration $x_c \sim 10\%$, when the average dopant distance equals the soliton width. Fukuyama *et al.*⁷ used a similar treatment by assuming suppressed dimerization at the doping site. As noted above, the SP LRO is destroyed by only 2% Zn doping albeit SRO SP phase persists up to 10%⁸. The simplest explanation that comes to mind would be something similar to non-magnetic dilution of 3D magnetic system. However, as noted above, 2% doping is far too low for a system to approch a simple percolation threshold unless there is extra mechanism which enhances severing the connections of different sites.

We point out that the essential physics which has gen-

erally been ignored in the theoretical treatment is the competition between the two degenerate SP ground state, due to this competition, SP phase is destroyed far before a simple percolation threshold is reached. Instead of simply cutting the interaction paths between next nearest neighbor spins in a standard percolation problem, the non-magnetic dopant in CuGeO_3 generates destructive quantum coherence which would induce the competition of the two dimer configuration(two ground states). Using a pseudo-spin model, it corresponds to inducing competing interactions or competing fields. Indeed, the intrinsic competing fields or interactions would drastically alter the phase behavior and push down the percolation threshold. Although a thorough numerical determination of the phase diagram is beyond experimentalist's scope, we can quantitatively explain the main issues of doped CuGeO_3 in this scenario. We argue due to the existence of competing field or interactions, there are two energy scales relevant in the doping problem, the first is related to the soliton width, which determines even the SRO SP phase is destroyed, it emphasizes the competition between SP and Néel phase. The second is related to the ratio between soliton creation energy to the interchain confining potential which determines where the system can still keep in LRO phase. This energy scale determines the competition between the two ground states. As first argued by Harris *et al.*¹⁴, the SP system can be mapped onto an effective 3D Ising model, in which the two dimer configurations possible in a given chain are associated with the up and down states of the Ising spins. When a Cu atom is replaced by Zn in an isolated chain, it is energetically favorable for the Ising pseudospin to change sign across the impurity across the Zn ion because the presence of the Zn ion makes the one of the original dimer configuration energetically unfavorable. Concomitantly, because the interchain interaction favors all pseudospin-up(or all pseudospin-down) configuration, introduction of impurities creates frustration in the 3D system. The theoretically challenging problem lies in mapping the effect of the dopant into the pseudo-Ising model. In Fig. 14, we show that the dopant effect can be simply mapped as an antiferromagnetic bond. We noticed a similar mapping by Mostovoy *et al.*, in which the equivalent fields are taken as infinite in solving the model, we believe this treatment in some sense blurs the underlying physics because the magnitude of the random bond is undoubtedly an essential energy scale of the system.

By taking the dopant effect as an antiferromagnetic bond, the resulting pseudo-spin model is 3D Ising system with mixed ferromagnetic and antiferromagnetic bonds. A diluted magnetic system with competing ferro- and antiferromagnetic interactions is the prototype of spin glass. But depending on the relative population of the ferromagnetic bonds and antiferromagnetic bonds, there could be a LRO ferromagnetic order below some critical concentration x_c which corresponds to SP LRO in our case. In the following, we explain how to interpret the experimental observations based on our model. First, we

can easily explain the low critical concentration which is the natural consequence of the competing interaction or fields. In a simple dilution problem, the dopants simply cut the connections of the magnetic interaction path and the percolation threshold is reached only when there is no longer a infinitely connected interaction network. In systems with competing interactions or fields, there is extra mechanism at play, which is the competition of the two ground states(Ising case). A simple account of this is as following: instead of just overcoming the dopant induced disconnections in the interaction path, one of the dimer configuration has to overcome the competition from the other one. Since locally the simple dimer configuration such as all spins up or spins down cease to be most energetically favorable. So two interpenetrating networks of the two dimer configurations has to compete with each other in achieving a infinite correlated network. A simple example is the short-range interaction system with evenly populated ferro- and antiferromagnetic bond, there is no appearance of LRO upon lowering the temperature. The percolation problem with competing interactions has been well addressed in conventional spin-glass systems²⁴, we simply borrow the scheme proposed by Maletta and Aeppli. Based on the competition between the Ferromagnetic LRO and spin glass, Maletta-Aeppli proposed a phenomenological cluster spin-glass model to explain the evolution from magnetic LRO to SG, by combining the percolation theory with the spin-glass picture, they suggest an effective decomposition of the spin system into spin-glass like and ferromagnetic networks. The spin-glass like network does not participate in the LRO, thus effectively cut the interaction path which lead to the LRO. We believe this picture can reasonably explain the low percolation threshold occurred in the doped CuGeO_3 case.

Second, by accepting the presence of intrinsic competing interaction or fields, we can naturally explain the anomalous phase behavior of doped CuGeO_3 in the context of well studied random field systems. So the SP transition in our phenomenological view occurs in a series of steps, first due to the one-dimensional nature of the system, the dimerization is established locally, due to the presence of the dopants and absence of the intra-chain interaction, the energy-minimum configuration would comprise of evenly populated two dimer configurations, as shown in *a*) of Fig. 13. Since the dopants cut the chains into even segments and odd segments, the even segments can easily pick the dimer configuration which can naturally pair up all the spins, this configuration has lower energy in comparison with the other one which has to create two solitons at the end of the segments. For the odd segment, the situation is different, the two dimer configurations are energetically equivalent because a soliton has to be created no matter what pairing is adopted. Accordingly to numerical simulations, the soliton in the odd segments should always be sitting in the middle, which, as we recall, would cut the odd segments into two smaller segments with opposite dimer orders. As temperature low-

ers, when 3D interaction becomes more and more important, a uniformly ordered phase is much more preferred, in doing so, the interchain interaction would prefer to keep all the dimers in phase which competes with the locally 'wrongly' ordered dimers, the resulting phase configuration is the compromise of these two effects, due to the presence of the competing interactions, the free energy landscape would be much more complex than system without competing interactions, there would exist numerous local minima which has extremely close energy with the true ground state although the configuration could be totally different, the complexity and presence of the local minima can easily explain the anomalous phase behavior observed in the experiments, as noted above, the final spin configuration results from competition between the tendency to totally disordered in the absence of the 3D interaction, or uniformly ordered in the absence of the 1D competing interactions. the variation in relative importance of these two factors would result in different ground states. This can naturally explain the complex phase behavior when the system is cooled through the transition temperature. Above the transition temperature, the system is mainly 1D correlated, the 3D interactions plays a negligible role, the system is then locally ordered without global coherence. When the temperature is lowered, the 3D interaction becomes more and more important and thus prefer the system to achieve a more ordered state. However, since there exists numerous local minima in the free energy scales, the system can easily fall out of equilibrium and be trapped inside a local minimum and remains in a metastable state, the relaxing process toward the true ground state would involve overcoming all the energy barriers in the energy landscape, if the relaxation time exceed the experimental measureable period, the system would remain in a non-equilibrium state forever, this is exactly what we have experimentally observed. In cooling from high temperatures, the system develops a symptomatically slow approach towards the LRO, anomalous slow dynamics, serious rounded phase transition can all be accounted for in the scenerio of competing interactions. At small dopings, the system actually acquires LRO and if waited long enough at each temperature point, there would exist no observable hysteresis between the heating and cooling run, as compared to a normal random field system, where hysteresis is usually observed²⁰. The non-Lorentzian scattering lineshape at high doping levels provides additional support for the competing interaction interpretation.

Another complex issue concerning the doped CuGeO₃ problem is the coexistence of the SP state and the Néel state. First discovered in magnetic susceptibility measurement, it has been believed the SP state and Néel state are exclusive to each other. Several features of the Néel state are woth mentioning: first, the Néel state is long range ordered or at least above the resolution of neutron scattering. Second, the magnetic ordering process shows considerable disordering like behavior, this has been revealed by both magnetic susceptibility study and neutron

scattering. The magnetic susceptibility measurement revealed the Néel transition to be very sharp at low and high doping levels but broadens substantially at the intermediate doping concentrations. In another study by Masuda *et al.*¹⁸, the broadening is interpreted as two separate Néel transitions. A subsequent neutron scattering on the same series of samples produced silimar results, in which the onset of the Néel state is seriously rounded in the intermediate range. The sample imhomogeneity has been excluded as the cause of the broadening¹⁵ since even higher doping samples shows much more clear transition. The nature of the conexistence has been addressed both by Khomskii⁶ and Fukuyama⁷. Both studies assumed a imhomogenous coexistence between the two competing ground states. *i.e.*, a suppressed dimerization near the doping site and enhanced ordering magnetic moment. This picture can natually explain the coexistence and the nominally exclusive ground states and the unconventional onset of the Néel state. More surprises turn up in the study of the low temperature phase behavior of the SP state on both Mg and Si doping studys. As would be discussed in detail in a separate paper¹³, we observed at approximately the same temperature of the onset of the Néel ordering, the SP phase undergoes a reentrant transition which is evidenced by the broadening in the dimerization peak width upon cooling through Néel transition temperature.

Furthermore, the reentrant process is accompanied again by slow dynamics and possibly even with hysteresis. The reentrance and the hysteresis are unusual in the sense it coincides with the onset of the Néel ordering over the doping range we studied, which implys the reentrance has direct relevance with the Néel ordering, a tricritical point theory can then naturally be excluded⁶. Another possible alternative would be the existence of a first order phase boundary between these two states, which would implicate the SP LRO is destroyed as soon as there is arbitrary small doping since experimentally people observed no lower critical concentration for the emergence of the Néel state. In Fig. 14, we show that a phase separation mechanism would be more reasonable in explaining the experimental observations. As we can see that solitons bear double idenities in the system, it is both structural anti-phase domain walls for the SP phase and the free spins for the underlying magnetic system, as noted above, below the SP transition while above the Néel transition, the interchain interactions plays more and more important role by creating a uniformly LRO SP phase, in which two solitons at the end of the segments would be created for even segments with out-of-phase ordering with the global ordering, or the already present soliton in odd segments would be bound to the dopant on one side to make the ordering in the segment in phase with the global odrdering, by doing so, a LRO SP order is achieved with lots of solitonscreated binding to the dopant sites, these free spins would generate decaying antiferromagnetic correlations among them, the SP ordered spins have been partially polarized in mediating the mag-

netic interaction. Below the Néel transition temperature, the spins develops antiferromagnetic order. We believe the key in inducing the reentrance is the non-uniform nature of the Néel state. Above the Néel transition, the free spins are disordered. However, when the system is cooled through the Néel transition temperature, the antiferromagnetic interaction energy would become relevant. The free spins are actually mobile and can move freely in each segments, it is only due to the confining potential of the interchian interation, all the soliton are then bound to the dopants, the onset of the Néel state, on the other hand, would compete with this configuration because, the lowest energy state would be achieved by moving all thses solitons together, in other word, phase separation into soliton-rich and soliton-poor region, which would inevitably disrupt the originally established SP order. We believe the resulting state is again the competing result of the SP order and Néel order, since the solitons are additionaly bound by the dopants, so the phase separation can happen only locally. We don't know now exactly whether the resulting state is something similar to islands or stripes(of course, eventually the Néel state is LRO, the island picture only means the LRO originates from islands or stripes), further theoretical work has to be done in this direction. But the slow dynamics and reentrance can naturally be explained in this way. Using this phase seperation picture, we would assume that, the SP phase might be irrelevant with the occurence of Néel phase in the sense that the integrated intensity of the SP phase would remain the same below the Néel transition temperature, it is only due to the inhomogeneity of the transition of both phases, that phase of certain SP ordered segments to be reversed. So it remains possible that the SP phase and Néel could still be independent identities, which of course, is against the main stream of theoretical interpretation right now.

VI. CONCLUSION

We have reported a comprehensive synchrotron x-ray and magnetic susceptibility study of the diluted SP material $\text{Cu}_{1-x}\text{Zn}_x\text{GeO}_3$, due to the high Q resolution and flux of synchrotron x-ray, we are able to carefully study the phase behavior of Zn doped CuGeO_3 , in agreement with Mg-doped CuGeO_3 , we confirmed the unconventional second-order phase transition for Zn-doped CuGeO_3 , in which two characteristic temperature are needed to describe the phase transition, T_m indicates the onset of the magnetic gap and also the metastable behavior, but system doesn't achieve LRO until T_{SP} , the unusual characters have been explained by the competing interactions or fieldls intrinsic to the doped system, a phenomalogical cluster spin glass picture percolation theory has been proposed to explain the phase diagram which gives a reasonable explanation for the both the critical concentration and the high doping concentration

phase behavior, combining information from both x-ray scattering and susceptibility measurements, we can conclude the unusual character for the Néel transition is unavoidably the direct consequence of the unconventional SP transition.

VII. ACKNOWLEDGMENTS

We are grateful to T. Masuda, K. Uchinokura, G. Shirane for important discussions and fruitful collaboration in the last several years. This work was supported by the NSF under Grant No. DMR97-04532.

TABLE I. Characterization of all samples

Zn(nominal) x(%)	Zn(EPMA) x(%)	Crystal weight (g)	SP T_{SP}	AF T_N	1.5
0	< 0.003	0.049	14.10	-	10.1
0.5	0.007 \pm 0.001	0.064	13.5	-	10.256
1	0.011 \pm 0.001	0.130	12.7	-	-
2	0.02 \pm 0.001	0.051	10.5	2.2	45
3	0.0235 \pm 0.001	0.043	9.7	2.75	4.17
3	0.027 \pm 0.0015	0.085	9.	3.1/3.8	8.7
4.3	0.0255 \pm 0.001	0.066	9.2	2.9	15.5
4.6	0.034 \pm 0.003	0.083	-	4.3	0.43
5	0.038 \pm 0.002	0.119	-	4.4	0.0037
6	0.038 \pm 0.005	0.020	-	4.4	-

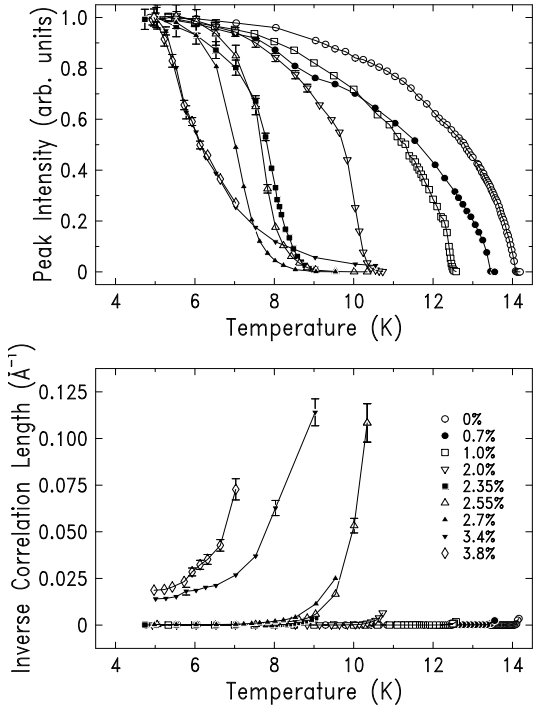


FIG. 1. The (1.5, 1, 1.5) SP peak intensity (a) and the corresponding inverse correlation length (b) as functions of temperature for various Zn-doping concentrations. Inset shows impurity-concentration dependence of the low-temperature SP inverse correlation length

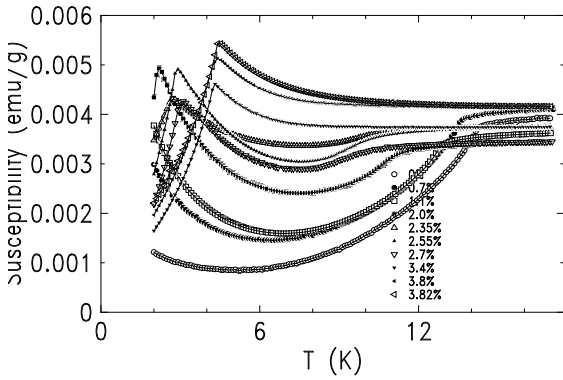


FIG. 2. The magnetic susceptibility as functions of temperature for various Zn-doping concentrations.

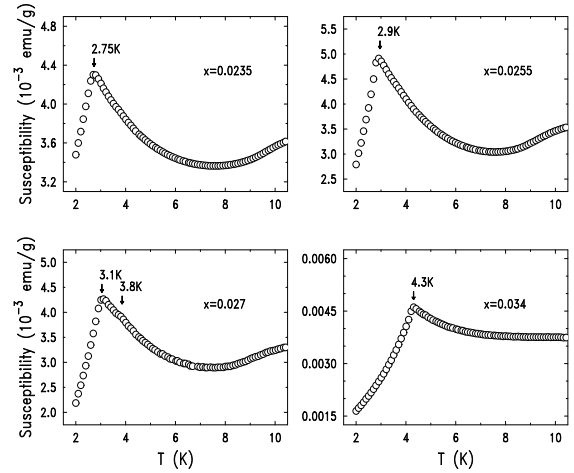


FIG. 3. The magnetic susceptibility for doping concentrations near critical concentration.

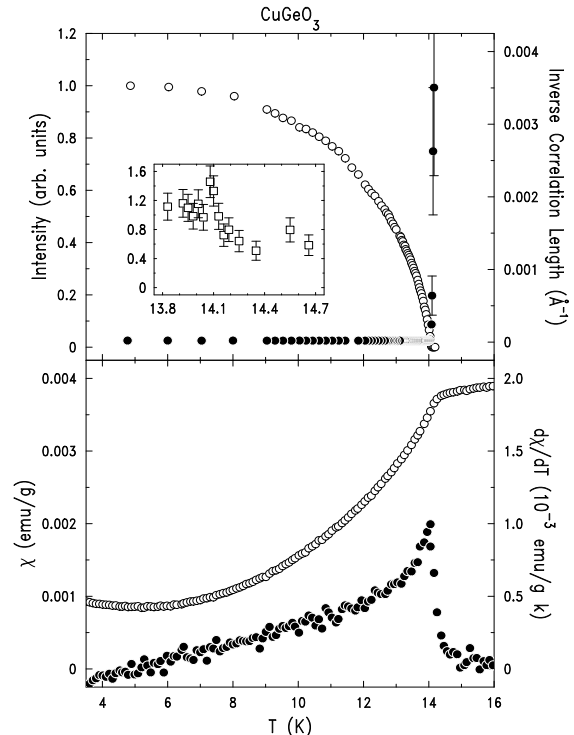


FIG. 4. (a) Intensity of the SP peak and inverse correlation length of the longitudinal scan as a function of temperature for pure CuGeO_3 , inset shows the critical scattering intensity at the wing of the superlattice peak (b) Magnetic susceptibility and temperature derivative of the magnetic susceptibility as function of temperature

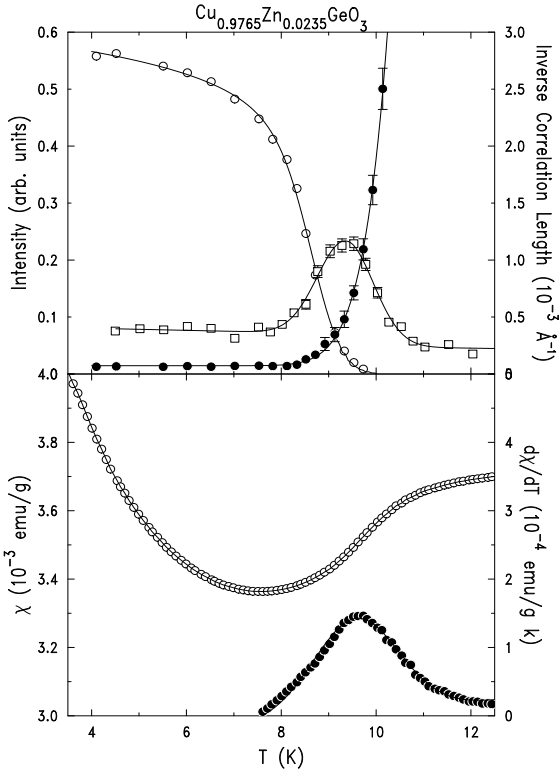


FIG. 5. (a) Intensity of the SP peak and inverse correlation length of the longitudinal scan as a function of temperature for $x=0.0235$ Zn doped CuGeO_3 , inset shows the critical scattering intensity at the wing of the superlattice peak (b) Magnetic susceptibility and temperature derivative of the magnetic susceptibility as function of temperature

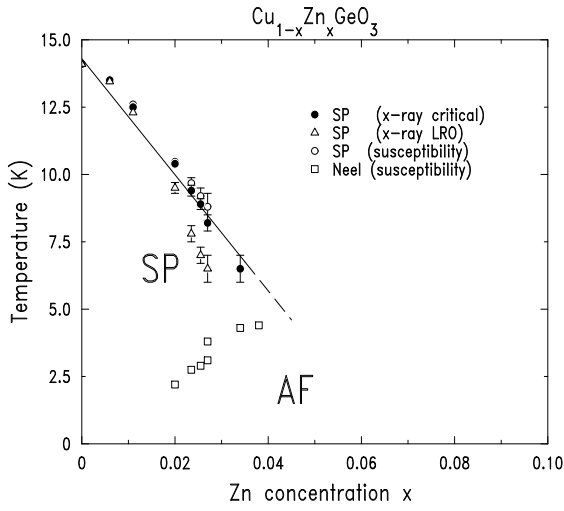


FIG. 6. T-x phase diagram of Zn-doped CuGeO_3

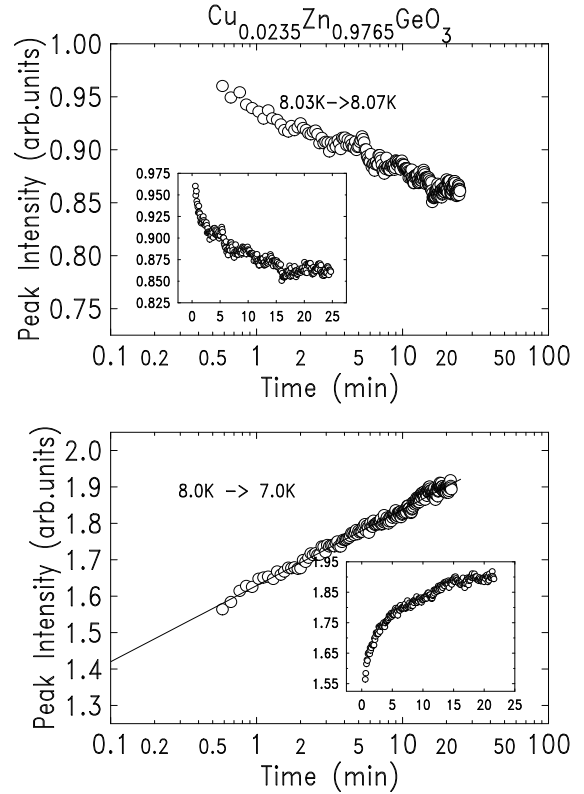


FIG. 7. (a) Semi-logarithmic plot of peak intensity of the superlattice peak as function of time after temperature change from 8.03K to 8.07K for 0.0235 Zn doped CuGeO_3 , inset shows the same data in normal scale (b) Semi-logarithmic plot of peak intensity of the superlattice peak as function of time after temperature change from 8.0K to 7.0K for 0.0235 Zn-doped CuGeO_3 , inset shows the data in normal scale.

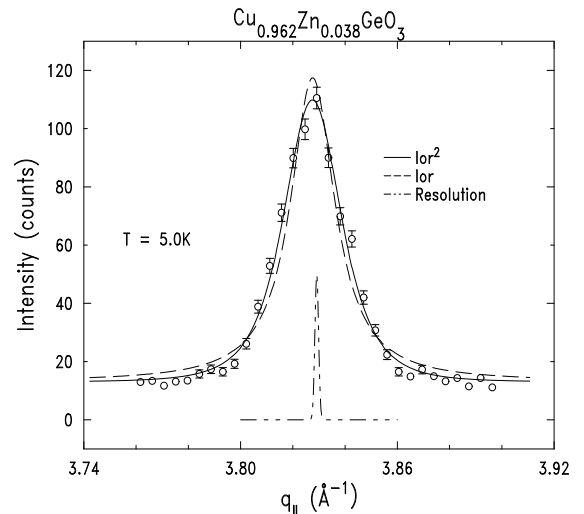


FIG. 8. Longitudinal scan profile of the superlattice peak at 5k for $x=0.038$ Zn doped CuGeO_3 , solid and dashed line shows the corresponding fitting by Lorentzian and Lorentzian squared lineshape convoluted with the resolution

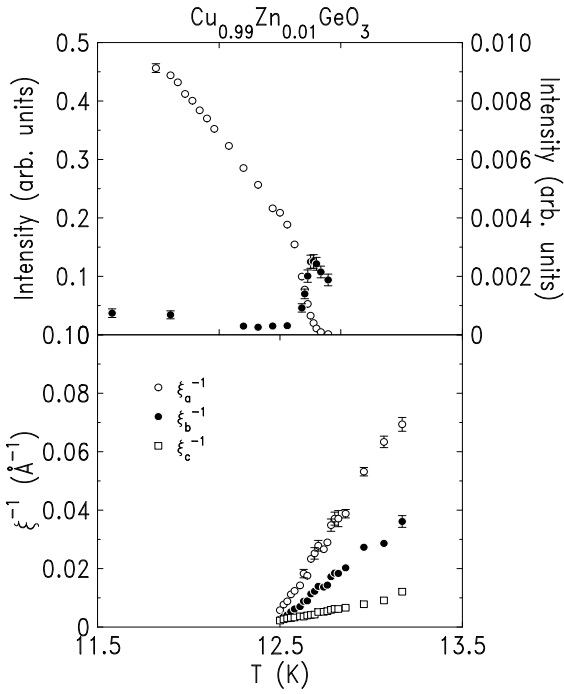


FIG. 9. (a) peak intensity of the superlattice peak and critical fluctuation at the wing as function of temperature for $x=0.01$ Zn-doped CuGeO_3 . (b) Inverse correlation along H, K, L direction of the critical scattering for $x=0.01$ Zn doped CuGeO_3

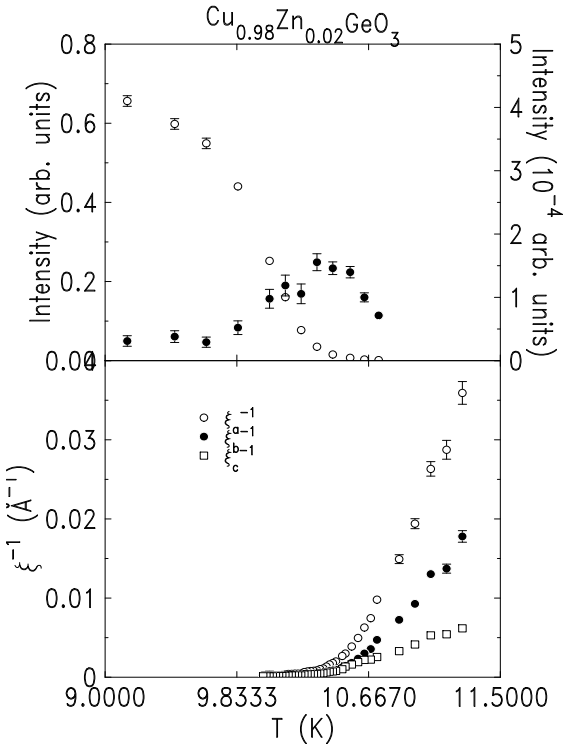


FIG. 10. (a) peak intensity of the superlattice peak and critical fluctuation at the wing as function of temperature for $x=0.02$ Zn doped CuGeO_3 . (b) Inverse correlation along H, K, L direction of the critical scattering for $x=0.02$ Zn doped CuGeO_3

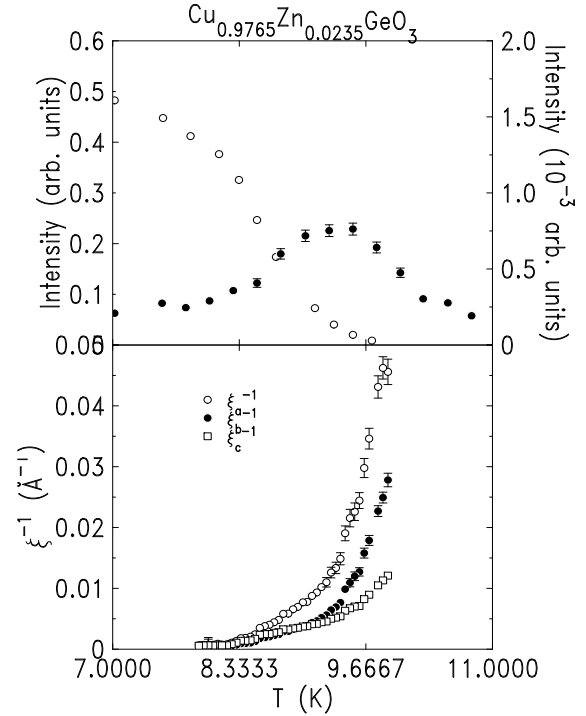


FIG. 11. (a) peak intensity of the superlattice peak and critical fluctuation at the wing as function of temperature for $x=0.0235$ Zn-doped CuGeO_3 . (b) Inverse correlation along H, K, L direction of the critical scattering for $x=0.0235$ Zn doped CuGeO_3

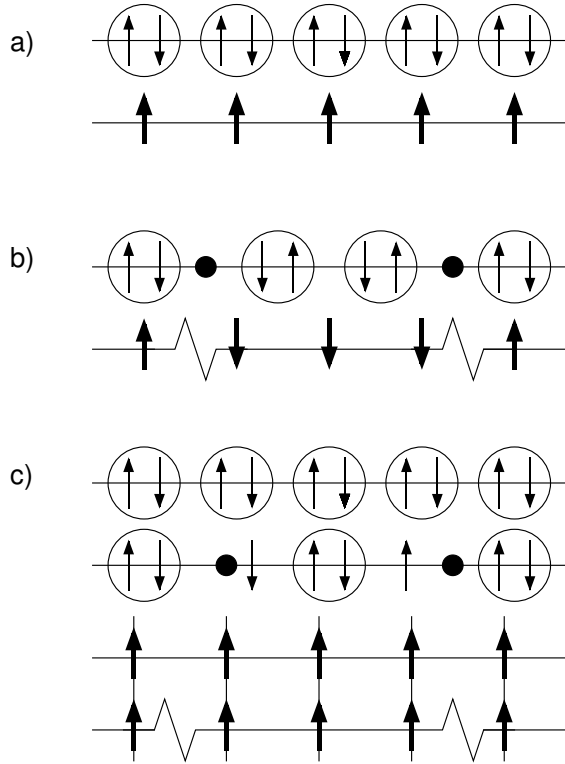
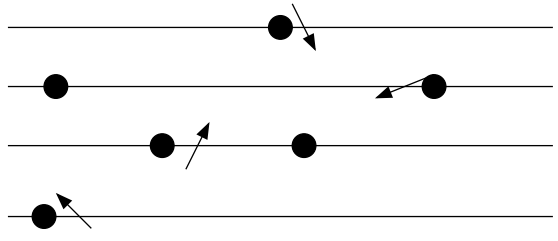


FIG. 12. (a)pseudo-Ising model for single chain without dopant (b) Pseudo-Ising model for single chain with dopant (c) Pseudo-Ising model including interchain coupling

$$T_{\text{Néel}} < T < T_{\text{SP}}$$



$$T < T_{\text{Néel}}$$

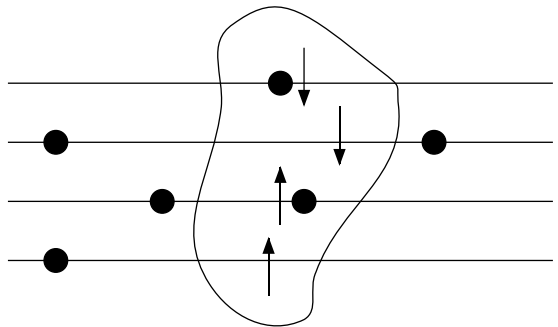


FIG. 13. (a)The free spin configuration above Néel transition(b) Antiferromagnetically ordered islands below Néel transition

¹ M. Hase, I. Terasaki, and K. Uchinokura, Phys. Rev. Lett., **70**, 3651 (1993); M. Hase, I. Terasaki, K. Uchinokura, M. Tokunaga, N. Miura, and H. Obara, Phys. Rev. B **48**, 9616 (1993)

² M. Hase, K. Uchinokura, R. J. Birgeneau, K. Hirota and G. Shirane **65**, 1392 (1996)

³ J.-G. Lussier, S. M. Coad, D. F. McMorrow and D. McK. Paul, J. Phys.: Condens. Matter **7**, L325, (1995)

⁴ S. B. Oseroff, S-W. Cheong, B. Aktas, M. F. Hundley, Z. Fisk, and L. W. Rupp,Jr., Phys. Rev. Lett **74**, 1450, (1995)

⁵ J. P. Schoeffel and J. P. Pouget, G. Dhaleen and A. Revcolevschi, Phys. Rev. B**53**, 14971 (1996)

⁶ M. Mostovoy, D. Khomskii, Z. Phys. B **103**, 209 (1997)

⁷ H. Fukuyama, T. Tanimoto and M. Saito, J. Phys. Soc. Japan, **65**, 1182 (1996)

⁸ Y. Sasago, N. Koide, K. Uchinokura, Michael C. Martin, M. Hase, K. Hirota and G. Shirane, Phys. Rev. B **54**, R6835, (1996); Michael C. Martin, M. Hase, K. Hirota, and G. Shirane, Y. Sasago, N. Koide, and K. Uchinokura, Phys. Rev. B **56**, 3173, (1997)

⁹ T. Masuda, A. Fujioka, Y. Uchiyama, I. Tsukada, and K.

Uchinokura, Phys. Rev. Lett. **80**, 4566, (1998)

¹⁰ H. Nakao, M. Nishi, Y. Fujii, T. Masuda, I. Tsukada, K. Uchinokura, K. Hirota and G. Shirane, cond-mat/9811324

¹¹ for a review, see J. W. Bray *et al.* in *Extended Linear Chain Compounds*, ed. J. C. Miller (Plenum, NY, 1982)

¹² Y. J. Wang, V. Kiryukhin, R. J. Birgeneau, T. Masuda, I. Tsukada and K. Uchinokura, Phys. Rev. Lett **83**, 1676, (1999).

¹³ Y. J. Wang, in preparation.

¹⁴ Q. J. Harris, Q. Feng, R. J. Birgeneau, K. Hirota, G. Shirane, M. Hase and K. Uchinokura, Phys. Rev. B **52**, 15420, (1995).

¹⁵ B. Grenier, J.-P. Renard, and p. Veillet, C. Paulsen, G. Dhaleen and A. Revcolevschi, Phys. Rev. B **58**, 8202, (1998); B. Grenier, J.-P. Renard, P. Veillet, C. Paulsen, R. Calemczuk, G. Dhaleen and A. Revcolevschi, Phys. Rev. B **57**, 3444, (1998)

¹⁶ S. Coad, J.-G. Lussier, D. F. McMorrow and D. McK. Paul, J. Phys.:Condens. Matter **8**, 6251 (1996)

¹⁷ H. Nakao, M. Nishi, Y. Fujii, T. Masuda, I. Tsukada, K. Uchinokura, K. Hirota and G. Shirane, cond-mat/9811324

¹⁸ T. Masuda, I. Tsukada, K. Uchinokura, Y. J. Wang, V. Kiryukhin and R. J. Birgeneau, preprint submitted to Phys. Rev. B

¹⁹ S. Fishman, A. Aharony, J. Phys. C **12**, L729, (1979)

²⁰ R. J. Birgeneau, J. Mag. Mag. Mat. **177-181**, 1, (1998)

²¹ R. J. Birgeneau, R. A. Cowley, G. Shirane, and H. Yoshizawa, J. Stat. Phys. **34**, 817, (1984)

²² Y. J. Wang, Y. -J. Kim, R. J. Christianson, S. C. LaMarra, F. C. Chou, and R. J. Birgeneau, preprint cond-mat/0004363, accepted by PRB.

²³ T. Masuda, K. Ina, K. Hadama, I. Tsukada, K. Uchinokura, H. Nakao, M. Nishi, Y. Fujii, K. Hirota, G. Shirane, Y. J. Wang, V. Kiryukhin, R. J. Birgeneau, preprint submitted to Physica B

²⁴ G. Aeppli, S. M. Shapiro, H. Maletta, R. J. Birgeneau, H. S. Chen, J. Appl. Phys. **55**, 1628, (1984); G. Aeppli, S. M. Shapiro, R. J. Birgeneau, H. S. Chen, Phys. Rev. B **29**, 2589, (1984)

²⁵ see, *eg.* , J. A. Mydosh, *spin glasses: an Experimental Introduction*, (Taylor & Francis, London, 1993)

²⁶ R. J. Christianson, in preparation.

²⁷ Tai-Kai Ng , preprint cond-mat/9610016

²⁸ G. B. Martins, E. Dagotto, and J. Riera, Phys. Rev. B **54**, 16 032 (1996)

²⁹ D. H. Reich, T. F. Rosenbaum, G. Aeppli and H. J. Guggenheim, Phys. Rev. B **34**, 4956 (1986)

³⁰ K. Hirota, G. Shirane, Q. J. Harris, Q. Feng, R. J. Birgeneau, M. Hase and K. Uchinokura, Phys. Rev. B **52**, 15 412 (1995)

³¹ M. Hase, I. Terasaki, Y. Sasago, K. Uchinokura and H. Obara, Phys. Rev. Lett **71** ,4059 (1993)

³² O. Tchernyshyov, A. S. Blaer, A. Keren, K. Kojima, G. M. Luke, W. D. Wu, Y. J. Uemura, M. Hase, K. Uchinokura, Y. Ajiro, T. Asano, M. Mekata, J. Magn. Magn. Mater. **140-144**, 1687 (1995)

³³ J. E. Lorenzo, L. P. Regnault, S. Langridge, C. Vettier, C. Sutter, G. Grubel, J. Souletie, J. G. Lussier, J. P. Schoeffel, J. P. Pouget, A. Stunault, D. Wermeille, G. Dhaleen and A. Revcolevschi, Europhys. Lett. **45**, 45 (1999)

³⁴ Q. Feng, R. J. Birgeneau and J. P. Hill, Phys. Rev. B **51**, 15188 (1995)